Original Article

Journal of Drought and Climate change Research (JDCR)

Winter 2026, Vol. 4, No. 12, pp 73-102

10.22077/jdcr.2025.9798.1158

Evaluation of Karst Development and Karst Water Resource Potential in Drought Conditions Using Fuzzy Logic Model (FAHP) and Analysis Hierarchy Process (AHP): A Case Study, Kohgiluyeh and Boyer-Ahmad Province, Southwest Iran

Nasrollah Kalantari[1], Sajad Pourakbari[2*]

1,2- Department of Geology, Faculty of Earth Sciences, Shahid Chamran University of Ahvaz, Ahvaz, Iran.

*** corresponding author: sajadakbari66@gmail.com**

Keywords:
Kohgiluyeh and Boyer-Ahmad, Karstification potential, GIS, AHP, Fuzzy logic

Received:
21 Jul 2025

Revised:
23 Oct 2025

Accepted:
09 Nov 2025

Abstract

The primary objective of the current study is to produce karstification potentiality maps in the northwest of Kohgiluyeh and Boyer-Ahmad Province, Iran, through the innovative use of both fuzzy logic and AHP models as additional tools in hydrogeological research. The present study is conducted over a broad area in the northwest of Kohgiluyeh and Boyer-Ahmad Province, covering 1148 km². The study area is located in the northwest of the province and is crossed by two rivers, Shah Bahram and Taghar. Geographic Information Systems (GIS) and Remote Sensing (RS) are used to create two maps depicting the development of karstification, consisting of five classes that show karstification potentiality ranging from very high to very low. The extraction of these maps is based on the analysis of input data such as lithology, lineament density, elevation, slope, rainfall, temperature, drainage density, and vegetation cover. Weights are assigned to all these factors according to their relevance to karstification potential. Eventually, two maps based on a weighted spatial modeling system are created. The verification results show that the fuzzy logic model outperformed the AHP model for the study area. The results provide significant information, and the maps can be used by local authorities for groundwater exploitation during drought periods, protection of the quality of karstic water resources, and management. This approach offers an innovative solution to water scarcity challenges, with potential applications in similar global settings and conditions.

How to cite this article:
Kalantari, N. & Pourakbari, S. (2026). Evaluation of karst development and karst water resource potential in drought conditions using Fuzzy Logic Model (FAHP) and Analysis Hierarchy Process (AHP): A case study, Kohgiluyeh and Boyer-Ahmad Province, Southwest Iran. *Journal of Drought and Climate change Research* (JDCR), *4*(12), 73-102. https://doi.org/10.22077/jdcr.2025.9798.1158

Introduction

Karstified carbonate formations are among the most important water resources in the southern and western regions of Iran (Karimi et al., 2003; Ashjari & Raeisi, 2006). Karstification typically occurs in biogenic, biochemical and chemical sedimentary rocks, mostly in carbonate rocks such as limestone and dolomite (Johnson & Stieglitz, 1990; Groves & Meiman, 2005; De Waele et al., 2009) and also in sulphate rocks such as gypsum and anhydrite (Black, 1997; Calaforra & Pulido-Bosch, 2003). Characteristic karst landforms include solutionally-enlarged factures and channels (karren) as well as closed depressions of differing origins, structure and dimensions (dolines, poljes). Cvijic (1893) described dolines as "the diagnostic karst landforms" (Ford, 2007). Karst landscapes are characterized by fluted and pitted rock surfaces, shafts, sinkholes, sinking streams, springs, subsurface drainage systems and caves. The unique features and three-dimensional nature of karst landscapes are the result of a complex interplay between geology setting, climate condition, and biological factors over the long-time scales. Karst landscapes in which the dissolution of bedrock by water is the dominant geomorphic process characterize almost 20% of the continents, and more than a quarter of the Earth's population lives on or near karst areas (Ford & Williams, 2007). Karstification has many practical implications: Sinkholes in karst areas are geotechnical hazards for houses, streets, and other infrastructure (Field, 2010; Vigna et al., 2010); reservoirs and other hydraulic infrastructure in karst often exhibit leakage problems (Bonacci & Roje-Bonacci, 2008; Bonacci et al., 2009a); karst areas exhibit significant biodiversity at the surface, underground, and in groundwater-dependent ecosystems (Humphreys, 2006; Bonacci et al., 2009b); Karst aquifers are valuable freshwater resources but are highly vulnerable to contamination, as they consequently require special protection (Ravbar & Goldscheider, 2007). Deep karst aquifers are valuable geothermal resources (Goldscheider et al., 2010).

Carbonate karstic formations outcrop in about 23% of the Zagros Region (Ashjari & Raeisi, 2006). The age of these karst formations is related to the Cenozoic era. Karst in the Zagros zone, compared to such formations in other regions of Iran, has differences owing to the regularity of folding in Zagros and being comprised of carbonate and non-volcanic rocks, such that carbonate rocks make up 95% of the mountains (Maleki et al., 2009). Carbonate rocks

in Zagros are affected by tectonic insertion factors and cold climate with long rainfalls, which have caused the maturation and evolution of karst and have created many caves such as "Ali Sadr" and "Shapour" (Moghimi, 2010). Fractures made in carbonate rocks due to tectonic factors are a sequential phenomenon in the Zagros Mountains Chain and are substantially the first stage of karstification (Maleki et al., 2009). Desert land encompasses two-thirds of Iran's landmass, which is devoid of forests and green pastures. Such harsh environmental conditions and water scarcity have led the Iranian people to mostly rely on groundwater resources rather than surface water (Baghvand et al., 2010; Bastani et al., 2010; Nosrati & Eeckhaut, 2012). On the other hand, having knowledge of karstic water resources and potential mapping always requires sophisticated, costly instruments and methodologies as well. Remote Sensing (RS) and Geographic Information Systems (GIS) have proven to be useful tools in karstification potential mapping.

Taşci et al. (2025) used Geospatial and Multi-Criteria Analysis for Identifying Groundwater Potential Zones in the Oltu Basin, Turkey. Echogdali et al. (2022) used Geospatial and AHP based identification of potential zones for groundwater recharge in Haridwar District of India.

Antonakos et al. (2014) applied multicriteria analysis within GIS environment in order to produce a distribution map of site suitability for drilling new production boreholes in Korinthia Prefecture (Greece). Konkul et al. (2014) applied a similar method to map the hydrogeological characteristics and groundwater potentiality of Huay Sai area (Thailand) using potential surface analysis. Chitsazan et al. (2015) compared karst development in two main zones Keyno anticline (Zagros Range) and Shotori anticline (Central Iran) of Iran. They used isotopic, hydro chemical and geomorphological data and they concluded arid karst aquifers have different characteristics compared with, typical karst aquifers. Fu Yeh et al. (2016) presented the estimation of groundwater recharge using GIS approach and integrated five contributing factors: lithology, land cover/land use, lineaments, drainage, and slope can be pointed out.

In Iran, more than 70 % of the rural and nearly 50% of the urban populations depend on groundwater resources for meeting their drinking and domestic requirements (Rahmati, 2013). Unfortunately, water scarcity is common in several parts of Iran that is being exacerbated by human activities and global climate change

(Ghayoumian et al., 2007; Abbaspour et al., 2009; Ayazi et al., 2010; Zarghami et al., 2011; Hosseini et al., 2012; Neshat et al., 2013). It seems that such conditions are to some extent similar around the arid and semi-arid areas of the world.

This paper presents the study of karstification potentiality mapping of the wide area of northeast of Khuzestan province area (southwest Iran) with the contribution of Remote Sensing and Geographic Information System, which aims to establish a supplementary or amending tool in locating karstic developed area. For this reason, rainfall data, hydrogeological, geomorphological and geological data as well as both AHP and Fuzzy logic methods are used for preparing karstification potentiality finals maps. Furthermore, the reliability of karstification potentiality mapping is controlled by using hydrogeological and geomorphological data. Assessing the karstification potential will be helpful for decision makers in karstic water resources management and identifying suitable locations for drilling production wells.

Physical setting of the area

The study area is located in southwest Iran, in the region of Kohgiluyeh and Boyer-Ahmad, occupying an area of 1148 km2 (Figure 1). The geomorphological development of the region is characterized by mild to relatively high relief with altitudes ranging from 687m to 3485m. Climatologically, the study area falls in semi-arid to semi-humid temperate climatic condition with cold winters and moderate summers. The monthly minimum temperature average is 6.5°C in the January and monthly maximum temperature average is 26.9°C in the August. In the last 30 years, the mean annual rainfall has been 1220 mm and the most rainfall occurs from November to the end of April. Shah Bahram River and Taghar River which gathers almost all the runoff of the study area and have a total length of 35 km and 28 km respectively, dominates in the drainage network of the wider region.

Concerning its' lithology, it is subsumed in the folding Zagros zone and consists of alluvial deposits, shale, marl, gypsum, dolomite and limestone formations (Figure 1). The geological bedrock consists of shale and marl which are almost impermeable. Limestones and dolomites are 200-400m thick and their permeability factor due to the existence of intense karst phenomena and tectonics is high. The main aquifers are developed within limestones and dolomites and they cover major parts of the study area.

Geological setting

The geological settings are very important, especially the nature of the overlying and underlying units and the topography. From the geological point of view, the basin is located in the Zagros Fold Belt, which has a main NW-SE trend. The outcrops of the region are the sequence of the Zagros Mountains Chain and have an age equal to Alpine folding. The outcrop layers in the studied zone are comprised of geosynclines sediments of Zagros zone and the age of which is from the early Cretaceous to the present era. The outcrops are the result of Alpine orogeny; started from the late Triassic and continued to the end of Pliocene (Aghanabati, 2004). The geological formations in the region from old to new are shown in Table 1. The detailed lithology of these formations has been described by James & Wynd, (1965); Stocklin & Setudehnia, (1977); and Alavi, (2004). The area is dominantly covered by Asmari and Sarvak carbonate formations and the Asmari and Sarvak karstic litho-units over and under respectively lie the inherently impermeable Pabdeh-Gorpi units where the latter acts as a hydraulic barrier.

Table 1. The geological formations and its description in the study area.

Formation name	Lithology	Age	%Area in the region
Nirez	Limestone, Dolomite, Marl	Liass	0.04
Khami Group	Limestone	UpperJurassic-LowerCretaceous	4.5
Gadvan	Shale	Huaterivian- Barremian	1
Daryan	Limestone	Aptian-Albian	0.4
kazhdomi	Shale	Albian- Cenomanian	2.4
Sarvak	Limestone	Albian-Santonian	41
Gurpi	Marl and Shale	Santonian- Maastrichtian	5.2
Pabdeh	Marl and Shale	Paleocene	16.3
Asmari	Limestone and Dolomite	Paleocene-Miocene	19.5
Gachsaran	Marl, Gypsum/Anhydrite and Halite	early Miocene	2
Bakhteyari	Conglomerate	Pliocene	2
Recent alluvium	Alluvium	Pleistocene- Holocene	1.1

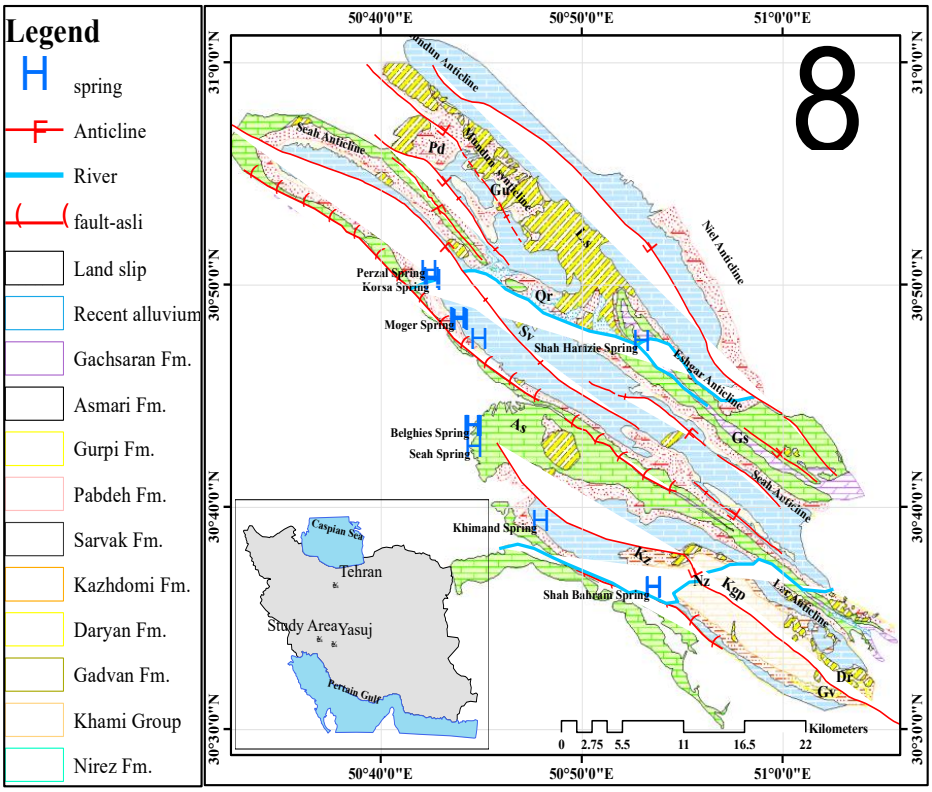

Fig 1. Location and geology map of the study area.

Tectonics and Structural Geology

The study zone is considered as part of Zagros folded region, which has a simple and gentle geological structure including sequences of close anticlines with usually vertical axial plane. The mountainous study area is characterized by intensive tectonic processes resulted in developed structural features such as anticlines, faults and fractures. Lithology and tectonic activities are the most important determinant of karst development occurrence in the study area. Structural features like Siah anticline, Lar anticline and Niel anticline, Mountain front fault trending NW-SE, parallel to the general structure of Zagros structural belt and Khark-Mish transverse fault are outstanding Structural features in the study area (Figure 1). Mountain front fault is one of the important faults, which have caused presence of Korsa karst spring with an average discharge of 1/3 m3/s the formation of other springs such as Perzal and Moger in the region are the result of the fault function possibly. Two major faults, the Mountain front and Khark-Mish faults, affect the study area. Different topographic, tectonic and geological evidences of the region indicate the same fact. In general, intensity of lineaments in Lar anticline is considerable and resulted

in the incidence of fracture frequency, intensive karstification and accordingly, facilitates groundwater movement. Geological and geomorphological structures play a key role in groundwater movement and similarly local and regional impact on flow pattern (Kalantari et al., 2011). The impermeable Pabdeh-Gurpi formation forms the core of the anticlines and groundwater moves on the top of this hydraulic obstruction.

Materials and Method

In order to conduct the present study, the following data and software are used: geological maps covering the study area (sheets: Deh Dasht, Sesakht, Fahliayn, 1:100,000 scale, source: Institute of Geology, 1967) meteorological and climatological data. Image processing software: ENVI 4.8. GIS software: ArcGIS 9.3. Expert choice 11 are being used. Geological maps of the study area were scanned, imported into ArcGIS 9.3 and georeferenced to the UTM/WGS84 projection system. Using ENVI 4.8 software, the bands of the satellite image were initially ‘‘layer stacked’’, and georeferenced, then the file was resized so that only the broader study area was included, then it was radiometrically corrected (log-residuals option) and finally a proper false color composite image was created. Then, creation of thematic maps took place, using lithology, lineament density, elevation, slope, rainfall, temperature, drainage density, and vegetation cover. A weighted spatial probability modeling was applied to identify karstification potential areas, according to their relevance to the development of karstification. Eventually, karstification potentiality maps were created, consisting of five gradational potentiality classes, ranging from very low to very high. The mathematical methods of Analytical Hierarchy Process (AHP) and Fuzzy logic, which were introduced by Saaty (1980) and Lotfizade (1965) respectively, were used to derive the final karstification potentiality maps. It should be noted that AHP method has been applied in many hydrogeological studies for site suitability analysis (Banai-Kashani, 1989; Pourghasemi et al., 2012). To do so, the individual karstification potentiality factors were given values (weights) according to their significance. In order to achieve this, all the factors were paired with each other and following that each factor was given an arithmetic value between 1 and 9, according to their significance when compared to the other factor with which it formed the pair (Table 2). Then, the karstification potentiality map was produced in accordance with

the mathematical equation 1 below:

$$M = w_1x_1 + w_2x_2 + w_3x_3 + w_4x_4 + w_5x_5 + w_6x_6 + w_7x_7 + w_8x_8 \quad (1)$$

Where *M* is the value for each pixel of the final karstification potentiality map of the study area. Variables w_1, w_2, w_3, w_4, w_5, w_6, w_7 and w_8 are the weight values for each preparatory factor and variables x_1, x_2, x_3, x_4, x_5, x_6, x_7, x_8 are the rating values for each pixel according to the preparatory factor to which it is referred (Domakinis et al., 2008). The quantitative parameters were classified according to the grading method of equal intervals of ArcGIS 10.2. This method has been used in the classification of hydrogeological studies as well as in the classification of vulnerability degrees (Huan et al., 2012; Kazakis & Voudouris, 2015). The eight factors for karstification potentiality mapping (lithology, lineament density, elevation, slope, rainfall, temperature, drainage density, and vegetation cover) are separately examined in the following paragraphs. The thematic maps portray the eight factors extracted for the calculation of the final maps. The values' range was reclassified based on different classes, with variable intervals (Table 2). The reclassification was performed based on the potentiality of karstification development. The factors' weights used are related to the participation of each factor on the karstification expansion. All maps were classified. The weights were adopted and optimized from the results of experience or judgments of experts in similar previous works on karstification potentiality mapping. The effectiveness (last column of Table 2) of each factor parameter is calculated by multiplying its weight by the rate (Al Saud, 2010). Factors with more value of effectiveness have more effects on karstification potentiality. Like the map prepared using the AHP method, the second map of karstification potentiality was prepared using fuzzy logic method and classified, and shown in Figure 6.

Table 2. Pairwise comparison matrix, factor weights and consistency ratio of the data Layers.

Weights	Rank	Parameter	Weights	Rank	Parameter
		Inverse Drainage density (Infiltration Density) (%)			**Rainfall (mm)**
0.077	2	25- 0	0.033	1	1200>
0.149	4	50 - 25	0.063	3	1450- 1200
0.261	7	75- 50	0.129	5	1700-1450
0.513	9	100 - 75	0.261	7	2000-1700
		Temperature (c)	0.513	9	2000<
0.532	9	5≥			
0.232	7	5-10			**Lineament density**
0.127	5	15-10	0.532	2	25- 0
0.068	3	20-15	0.232	4	50 - 25
0.040	1	20≤			
		Vegetation cover	0.147	7	75- 50
0.382	9	Dense forest	0.088	9	100 - 75
0.204	8	Dense grassland			**Elevation(m)**
0.142	7	Semi-dense forest	0.033	9	1000≥
0.096	6	Semi-dense grassland	0.063	7	1500-1000
0.065	5	Sprawling forest	0.129	4	2000-1500
0.053	4	Low-density grassland	0.261	2	2500-2000
0.037	2	Irrigated agriculture and orchards	0.513	1	2500<
		Formation name			**Slope(°)**
0.499	9	Asmari / Sarvak /Gachsaran	0.513	9	5≥
0.275	6	Daryan	0.261	7	5-10
0.129	5	Khami Group	0.129	5	15-10
0.063	3	Nirez	0.063	3	35-15
0.033	1	Gadvan / Kazhdomi / Pabdeh / Gurpi / Recent alluvium	0.033	1	35≤

Table 3. Matrix of factors weights evaluation

	(a)	(b)	(c)	(d)	(e)	(f)	(g)	(h)	Weights
Formation (Lithology) (a)	1	3	4	5	6	7	8	9	0.387
Lineament density (b)		1	2	3	4	5	6	7	0.209
Precipitation (c)			1	2	3	4	5	6	0.144
Elevation (d)				1	2	3	4	5	0.098
Vegetation cover (e)					1	2	3	4	0.066
Temperature (f)						1	2	3	0.044
Drainage density (g)							1	2	0.031
Slope (h)								1	0.022
									CI=0.04

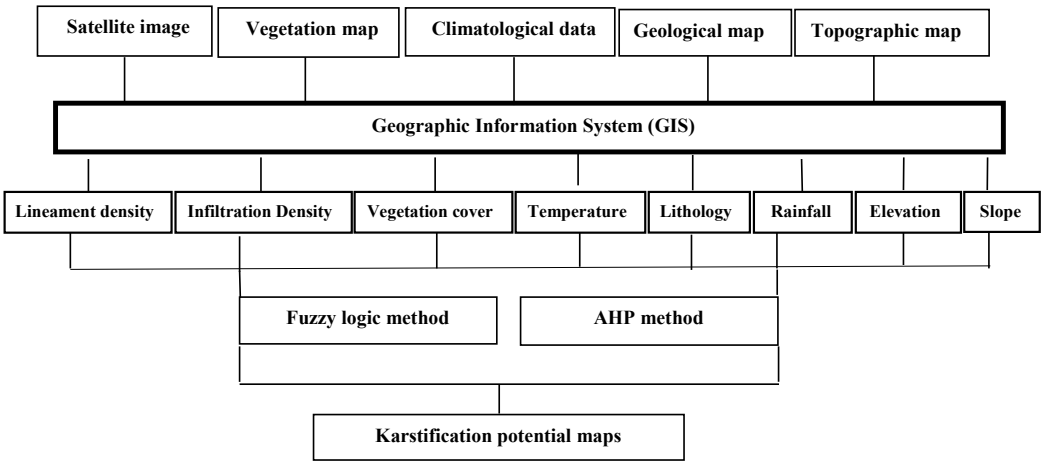

Fig 2. Flow chart of the methodology for assessing the karstification potential of the study area

Selecting thematic layers influencing karstification potential

The number of used thematic layers depends on the data availability in the study area. In order to assess karstification potential zones, eight thematic layers namely lithology, lineament density, elevation, slope, rainfall, temperature, drainage density, and vegetation cover are chosen as the effective factors. Hydrology conditions are largely dependent on these thematic layers and hence influence the occurrence of karstification. These thematic layers provide a reliable ground for an effective prediction of the karstification potential of a given area. The whole process of the karstification potential prediction is shown in Figure 2.

Factors influencing karstification

Formation (Lithology)

Lithology (Formation) factor (weight 38% or 0.38) is associated with water permeability and ability of the formations to host groundwater. Fracture systems, joins, dykes and porosity influence the capacity and specific storage of groundwater among various rock types. Along with primary porosity, sedimentary aquifers have higher capacity and specific storage of groundwater than the karst and fissured rock aquifers in which the groundwater interesting is locally and predominately in faults and fractures. The geological map was derived from the available geological maps with scale 1:100,000 from National Iranian Oil Company. Different Formations were digitized as polygons and thus the thematic map was produced. Consequently, the map of Figure 3a was created and divided into 11 classes. Shale, marl and siltstone are impervious geological formations

and create a barrier to groundwater infiltration while they have low storage capacity of groundwater. Other formations are including limestone, dolomite, gypsum and recent alluvium.

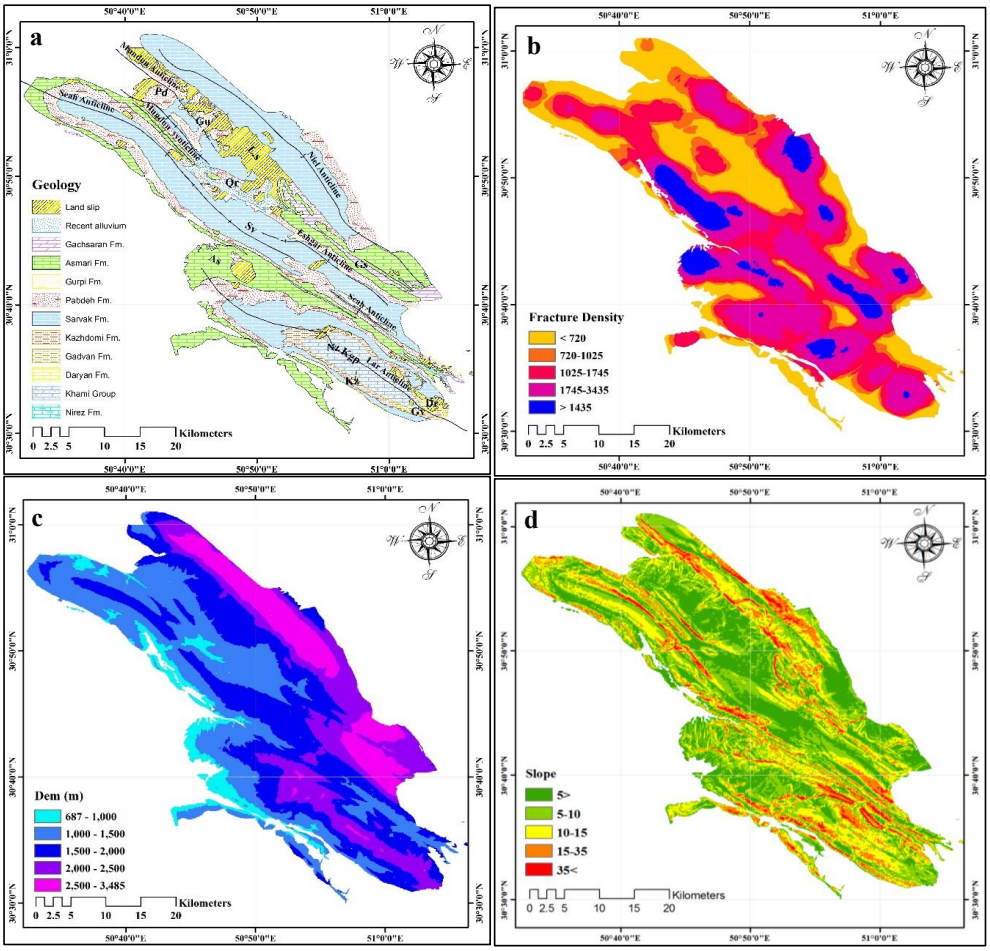

Fig 3. Continued on the next page.

Lineament density

A lineament is a linear feature in a landscape which is an expression of an underlying geological structure such as a fault. For the extraction of lineaments' density map, a satellite image Landsat-7/ETM^{+} was initially processed in ENVI4.7, in order to determine the most appropriate False Color Composite/FCC image for lineaments' delineation. Combination of bands 753: RGB (Red/ Green/ Blue) was proved to be the most suitable for this purpose. After the lineaments' (satellite image) and faults' (geological map) digitization, their density was calculated in Arc map 10.2 (Line Density command). Next, a reclassification of the raster lineament density file followed into 5 classes, from very low to very high, according to the class boundaries of Table 2,

yielding Figure 3b map. The lineament density raster file was assigned a weight of 20% (0.20) in the calculation of the karstification potentiality final map, according to AHP methodology. It should be noted that in the area of orange color, where no faults and lineaments exist, the potentiality of the karstification is low, in contrast with the Purple colored area, where the probability reaches its maximum level.

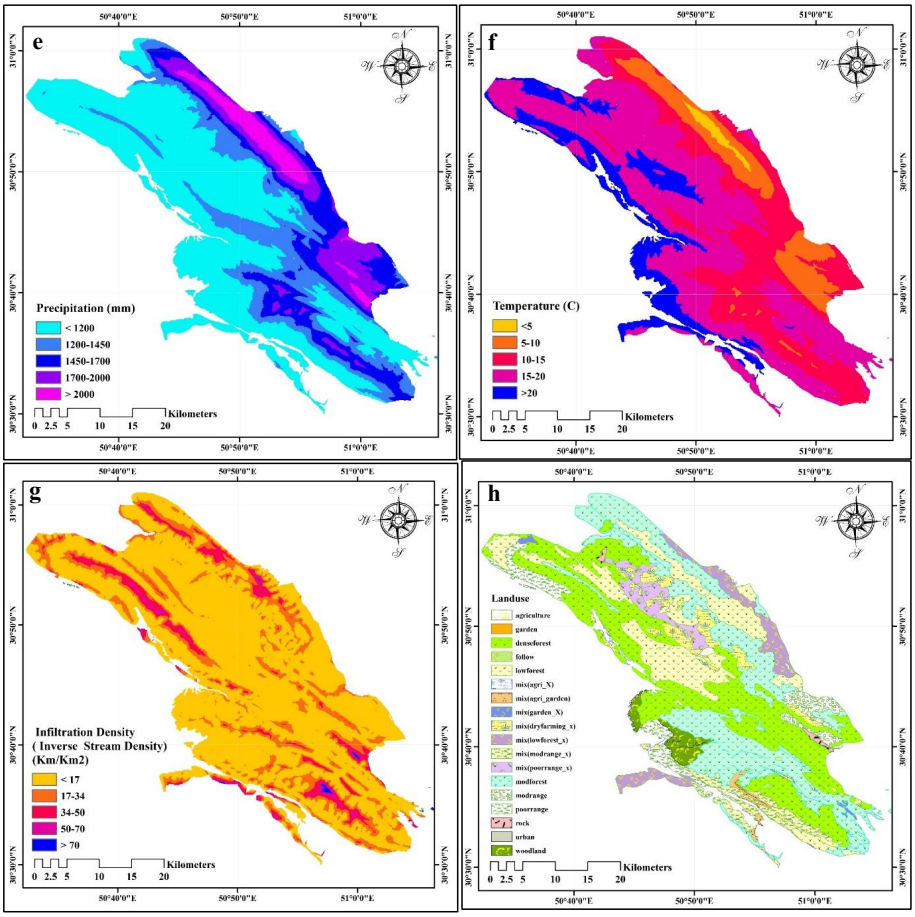

Fig 3. Maps of eight causal factors in karstification potentiality

Elevation

Elevation is one of the controlling factors in the karstification and was assigned a weight of 9% (0.09) in the final karstification potentiality value. Elevation influences to karstification are often displayed as indirect relationships or by means of other factors. In general, topography plays a key role in the recharge, discharge and emerges of karstic springs. With an increase in height in a region, due to increased hydraulic gradient, karst development potential will be increased. The Digital Elevation Model (DEM) was created from the available

topography maps with scale 1:250,000 from Institute of Geology and Mineral Exploration. The thematic map of elevation was divided into five classes with different ranges: a) 687- 1000 m, b) 1000-1500 m, c) 1500-2000 m, d) 2000-2500 m e) 2500-3487 m (Figure 3c).

Slope

Slopes were produced after the DEM in Arc Map 10.2. The values (in degrees) were reclassified into classes as shown in Table 2. In general, slopes rule the ability of surface water either to remain on the surface long enough to infiltrate or to continue to flow. Usually, the steep slopes indicate greater water velocity. Therefore, it is observed that in the areas of steeper relief, runoff is increased which in turn minimizes the degree of groundwater recharge (Doll et al., 2002). On the contrary, on the relatively gentle sloping terrains, the groundwater potentiality and karstification potentiality increases due to greater infiltration i.e. the lower the slope, the greater the recharge (Figure 3d). The slope factor was assigned a weight of 2% (0.02) in the calculation of the karstification potentiality final map, pursuant to AHP method.

Precipitation (rainfall)

This is one of the most important factors and was assigned a weight of 14% (0.14) in the final karstification potentiality value. The higher the precipitation, the higher the karstification potentiality will be. During the present study, monthly rainfall data were collected from 8 stations of the wider area in combination with the Digital Elevation Model (DEM). The mean annual rainfall ranges from 552 to 791 mm in the lowland areas, while in the mountainous areas, rainfall was identified with the altitude. A regression line indicates the following relationship between the rainfall (P in mm) and the altitude (h in m): $P = 0.722\ h - 17.5$. The above relationship was used to illustrate the rainfall map. The resulting map was classified into five major classes (Table 2 and Figure 3e): >2000 mm/yr (Very High), 1700–2000 mm/yr (High), 1450–1700 mm/yr (Moderate), 1200–1450 mm/yr (Low), and <1200 mm/yr (Very Low). From the rainfall map, it is observed that in comparison to areas of lower altitude, in areas with higher altitude and rainfall, greater potentiality of karstification exists. About 71–82% of annual rainfall occurs in 5-6 months (October-April next year), while summers are usually dry.

Temperature

Due to the role of temperature in

karstification, this data layer was created. The lower the temperature, the higher the karstification potentiality will be. During the present study, monthly temperature data are collected from 8 stations of the wider area in combination with the Digital Elevation Model (DEM). The mean annual temperature ranges from 2.4 to 23.4 C° in the study area. A regression line indicates the following relationship between the temperature (T in mm) and the altitude (T in C°): T = -0.0075h + 23.4. The above relationship is used to illustrate the temperature map. The resulting map is classified into five major classes (Table 2 and Figure 3f): >20C° (Very Low), 15– 20 C° (Low), 10–15 C° (Moderate), 5–10 C° (High), and <5 C° (Very High). This factor is given a weight of 4% (0.04) in this analysis.

Infiltration density (Inverse Drainage density)

Drainage density is the total length of all the streams and rivers in a drainage basin divided by the total area of the drainage basin. It is a measure of how well or how poorly a watershed is drained by stream channels. The drainage network of the study area was created from the DEM through a commands' sequence in ArcMap 10.2 and its density (Figure 3g) was calculated using the "Line Density" command. Next, a reclassification of the raster drainage network density file followed, into 5 classes, from very low to very high. The drainage network that was produced is of dendritic pattern, resultant by water flowing in a homogenous soils' surface. According to geomorphological knowledge, the denser the drainage is, the less the recharge rate will be and vice versa. Hence, the infiltration density map was extracted from the inverse drainage density map according to the class boundaries of Table 2. Therefore, in the blue areas, the potential for karstification is higher (Figure 3g). The raster infiltration density file was assigned a weight of 3% (0.03) in the calculation of the karstification potentiality final map, based on AHP method.

Vegetation cover

Vegetation cover controls the infiltration of rainwater into subsurface and recharge processes. Vegetation cover is an indicator for the suitability of groundwater prospect. In the high-density vegetation area, the surface runoff is slow allowing more time for rainwater to percolate, whereas low density vegetation area facilitate high runoff allowing less residence time for rainwater hence comparatively less

infiltration is there (i.e. Infiltration is straightly related to Vegetation cover). In this study, a single date image by Landsat ETM^+ is used to generate land cover types and is assigned a weight of 6% (0.06) in the final karstification potentiality value. The study area is divided into eight land cover classes (Table 2) (Figure 3h).

Analytical Hierarchy Process (AHP)

AHP is a multi-objective, multi-criteria decision-making approach which enables the user to arrive at a scale of preference drawn from a set of alternatives (Ayalew et al., 2005).To apply this approach, it is necessary to break a complex unstructured problem down into its component factors; arrange these factors in a hierarchic order; assign numerical values to subjective judgments on the relative importance of each factor; and synthesize the judgments to determine the priorities to be assigned to these factors (Saaty & Vargas, 2001). In the construction of a pair-wise comparison matrix, each factor is rated against every other factor by assigning a relative dominant value between 1 and 9 to the intersecting cell (Table. 2). When the factor on the vertical axis is more important than the factor on the horizontal axis, this value varies between 1 and 9. Conversely, the value varies between the reciprocals 1/2 and 1/9 (Table 3). In these techniques, firstly, the effects of each parameter to the occurring karstification relative to each other were determined by dual evaluation in determining the preferences in the effects of the parameters to the karstification potentiality maps. Normally, the determination of the values of the parameters relative to each other is a situation that depends on the choices of the decision-maker. Consequently, the weight values were accurately determined for the real land data (Table 2 & Table 3). In this study, spatial databases were used; the findings were obtained as a result of the field and office studies carried out to create karstification potentiality maps. The analysis of data layers converted to a raster data model was completed by determining their weights in terms of both data layers and sub-criteria, in consequence of the calculation carried out according to the AHP. For all the models, where AHP was used, the CR (Consistency Ratio) was calculated (Saaty, 1977). The models with a CR greater than 0.1 were automatically rejected. With the AHP method, the values of spatial factors' weights were defined.

Fuzzy logic

The idea of fuzzy logic is to consider the

spatial objects on a map as members of a set (Lotfizadeh, 1965). In classical set theory, an object is a member of a set if it has a membership value of 1, or not a member if it has a membership value of 0. In fuzzy set theory, membership can take on any value between 0 and 1 reflecting the degree of certainty of membership. Fuzzy set theory employs the idea of a membership function that expresses the degree of membership with respect to some attribute of interest. Working in GIS with map layers, generally the attribute of interest is measured over discrete intervals, and the membership function can be expressed as a table relating map classes to membership values. Fuzzy logic is attractive because it is straightforward to understand and implement. It can be used with data from any measurement scale and the weighting of evidence is controlled by the expert. Fuzzy logic method allows for more flexible combinations of weighted maps, and can be readily implemented with a GIS modeling language. When using fuzzy logic in karstification potential mapping, the spatial objects on a map are considered as members of a set. For example, the spatial objects could be areas on an evidence map (map of causative factors for karstification potential) and the set defined as ‘‘areas suitable to karstification accruing”. A variety of operators can be employed to combine the membership values when two or more maps with fuzzy membership functions for the same set are available. This study uses the fuzzy gamma operator for combining the fuzzy membership functions.

Final maps

After the procession of all aforementioned factors, the final maps of potentiality of karstification occurrence in the northwest of Kohgiluyeh and Boyer-Ahmad province were constructed applying two methods. The procedure followed is based on multiplying to the following equation; E being the final karstification potentiality value used in AHP and fuzzy logic methods:

E= 0.38 × Lithology + 0.20 × Lineaments and faults + 0.09 × Elevation + 0.02 × Slope + 0.14 × Rainfall + 0.04 × Temperature +0.03 × Infiltration density (Inverse Drainage network*)* +0.06 × Cover vegetation (2)

The resulting values were reclassified into five classes with karstification potentiality from very low to very high owing to the grading method of natural break (Figure 4 & Figure 6). This is attributed as: non karstic, low, moderate, high and very high. According to the final maps produced by AHP and fuzzy logic methods, the

area covered by the above classes was calculated and distribution of karstification potentiality classes in the study area shown in Figures 5 and 7. It appears that areas of high and very high potentiality produced by AHP method occupy an area of 459 km^2, while non karstic and low potentiality cover an area of in an area of 287 km^2. Moderate karstification occurs in an area of 401 km^2. These amounts about to fuzzy logic method are as follows: 138 km^2 (non karstic), 184 km^2 (low), 344 km^2 (moderate), 287 km2 (high), and 195 km^2 (very high). The lithological formations with the highest potentiality for karstification are the limestones in the study area. The high potentiality for karstification in the limestones is attributed to the high amounts of rainfall, fractures existing and potential recharge, in contrast with the alluvial and marl formation which are rendered to non karstic potentiality owing to their hydrogeological and morphological characteristics. The karstification potentiality map can be a useful tool in order to identify new supply sources for water. The proposed method is suitable for areas where carbonate rocks are characterized by high degree of karstification. However, the flexibility of this method allows the revision of the weights and rating of parameters in order for other regions to be suitable according to their specific characteristics.

Validation

Validation is the most important process of modeling in that without validation, the models will have no scientific significance (Chung & Fabbri, 2003). Validation of karstification potential map was done with the existence and location of springs, sinkholes and karst aquifers in the study area (Figure 4 & Figure 6). For this purpose, the evidences obtained from Google Earth images and aerial photographs of the study area, as well as field surveys were applied. The springs and sinkholes detected in this method, overlaid over the final output map of karstification prospect zones and it was found that high to very high karstification potential zones delineated in this research using RS and GIS tools with AHP and Fuzzy logic techniques coincide with sinkhole density (Which are directly responsible for the recharging groundwater area) and also the emergence of springs with considerable discharge rates (from 500 to more than 3000 lit/s), whereas in the regions delineated under moderate to poor karstification potential, no spring or sinkhole was detected. Additional uncertainties in mapping the spatial distribution relates to the compatibility between the scale and the resolution of

the mapping technique (Tweed et al. 2007). Although the high cost for the water transfer is the main reason for the absence of the borehole, it could be used as a backup water resource region for future use. Thus, the finding of this research establishes the accuracy of the techniques for karstification potential zone mapping and can be used for other regions having similar geological settings. Belqis, Khiemand and Korsa are three major springs in the study area that their catchment area located in high and very high karstification potential zones (Figure 8).

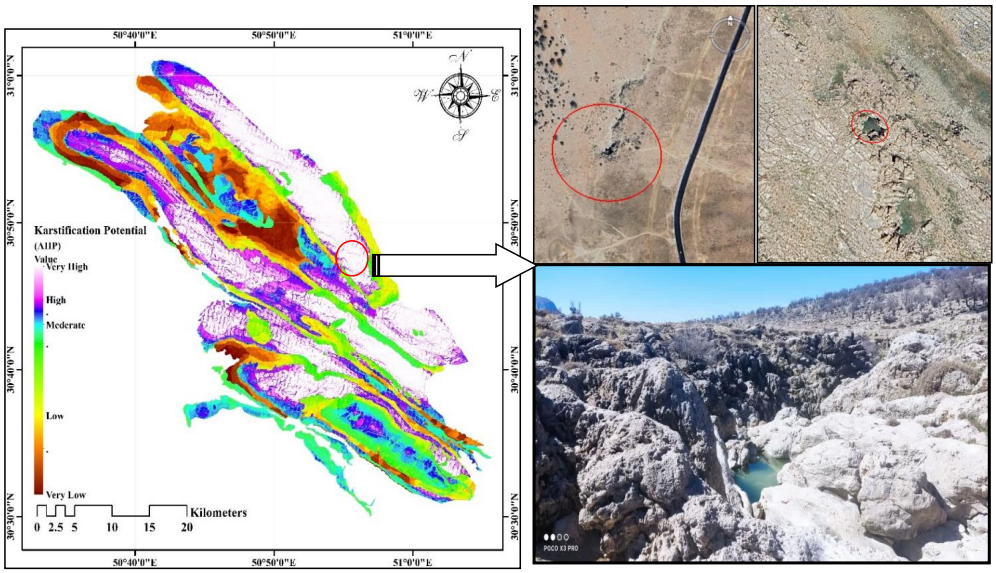

Fig 4. Karstification potential zones produced by AHP method and its validation of the study area.

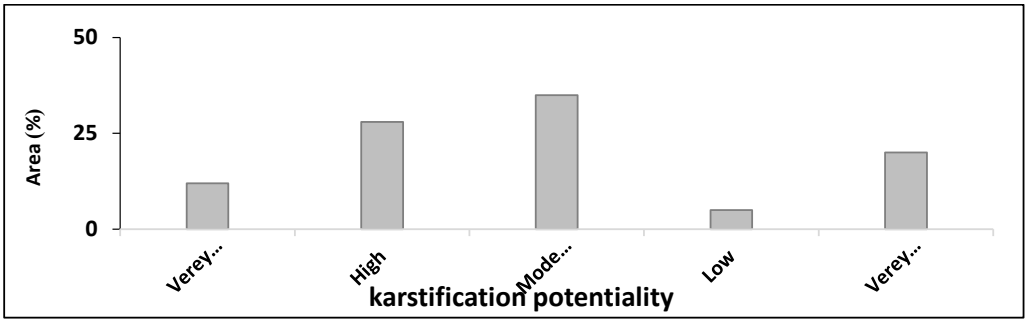

Fig 5. Distribution of karstification potentiality classes in the study area according to AHP Methodology.

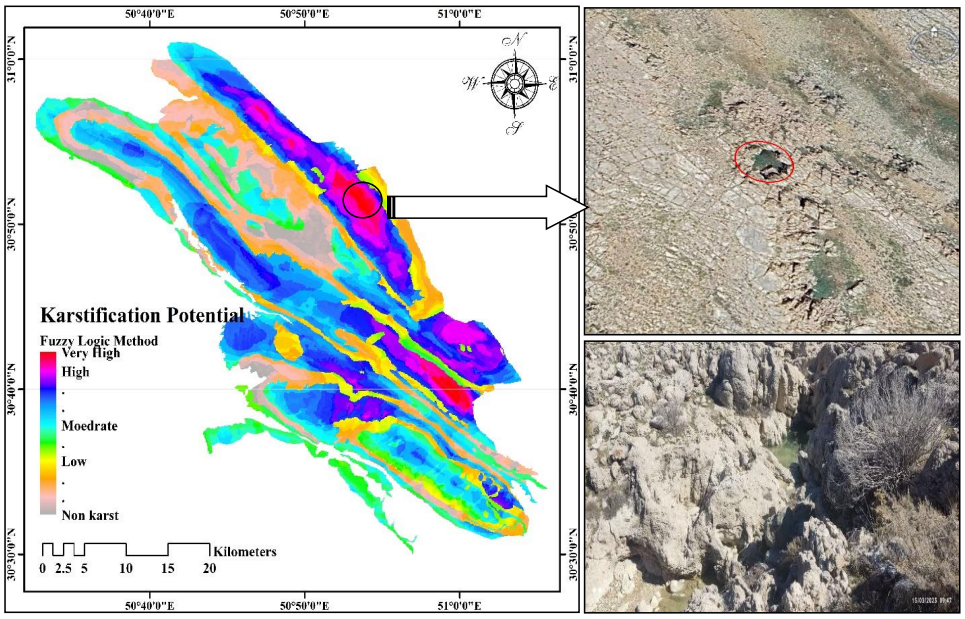

Fig 6. Karstification potential zones produced by Fuzzy logic method and its validation of the study area.

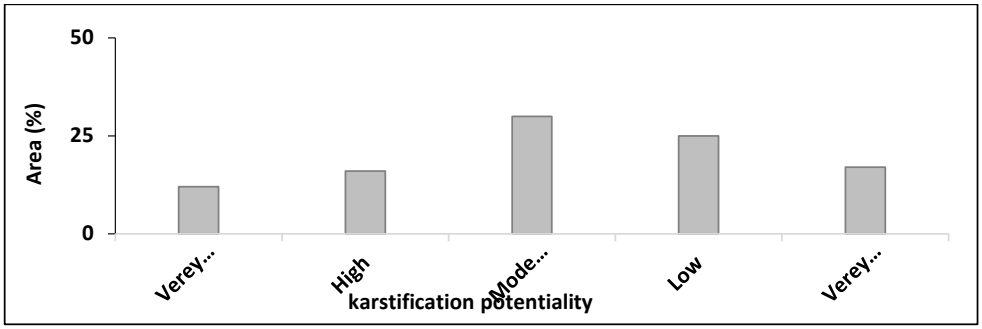

Fig 7. Distribution of karstification potentiality classes in the study area according to Fuzzy logic methodology.

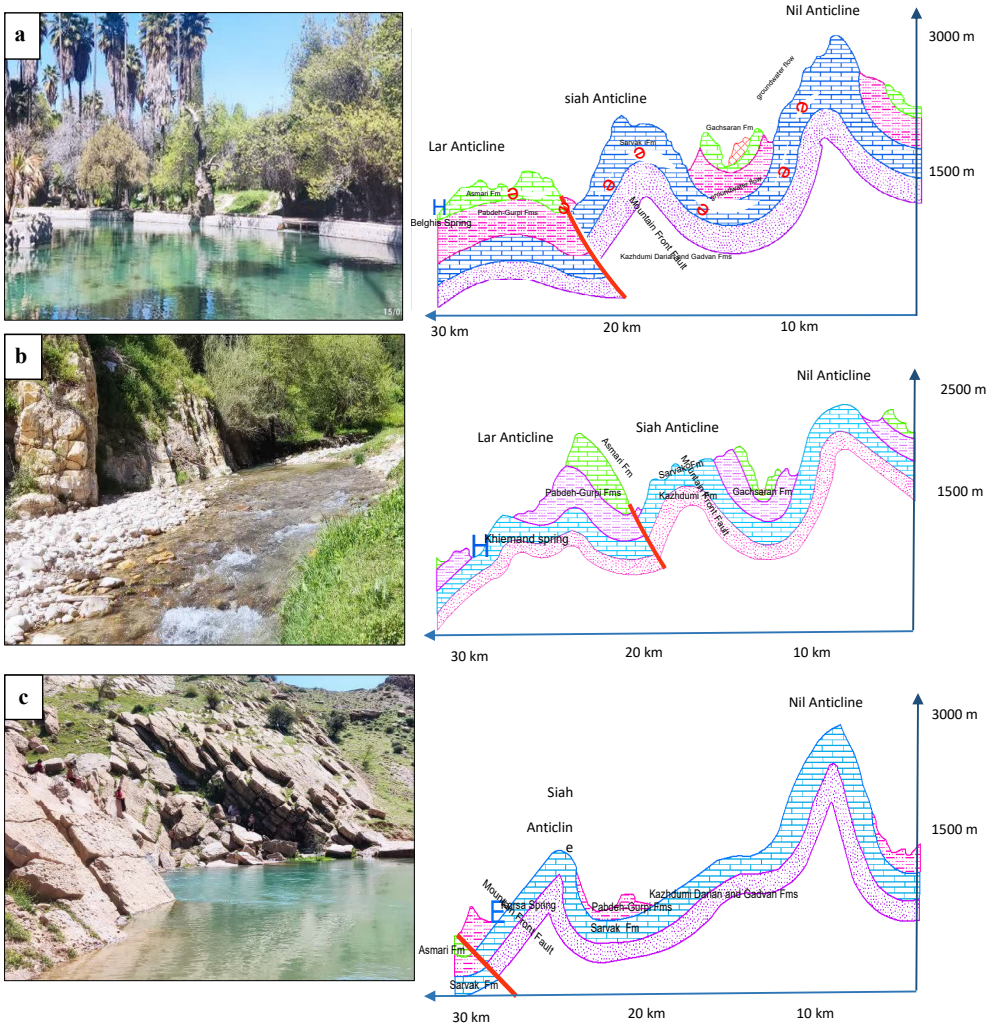

Fig 8. Karst springs and their cross sections in the study area Belqis (a), Khiemand (b), Korsa (c)

Hydrogeological characteristics

The karst springs in the study area represent natural exits for groundwater. Springs appear at the contact between fractured Sarvak limestone rock and low permeability Pabdeh formation (Khiemand and Korsa) and in the Asmari formation itself (Belqis).

The Korsa spring is considered as one of the indicators of the hydrogeological condition of the Sarvak Formation and the Black Anticline in the study area. The seasonal Korsa spring emerged from the Black Anticline and along the mountain frontal fault. According to the morphological evidence and the drawn structural sections, the Korsa spring is a contact-fault type spring. The outcrop of this spring is located along the transverse fracture. This spring is located on the line of the mountain frontal fault, and the presence

of this fault plays a significant role in the formation and upper discharge of the spring. The height of the spring emergence is 830 meters above the level of the open sea. The outlet of the Korsa spring is discharged as a fracture zone (Figure 8). This spring has very large discharge changes, which indicates the role of fractures and the presence of dissolution channels in the hydrogeological system of the limestone aquifer that feeds it. The spring discharge in the water year 2022-2023 fluctuated from 2.95 cubic meters per second in April 2023 to the spring drying up in July (Figure 9). So that the ratio of maximum discharge to minimum discharge was calculated to be 2.95 and its average was about 1.24 cubic meters per second. In rainy years, the maximum discharge also exceeds 6 cubic meters per second.

Belqis spring is considered representative of the Arend karst aquifer (northwestern ridge of the Lar anticline) with the limestone skeleton of the Asmari Formation. The spring is one of the large karst springs in the northwest of Kohgilobe and Boyer-Ahmad provinces. This is a manifestation of the fractured zone resulting from the action of the Khark-Mish basement fault and in the direction of the anticline plunge (Figure 8). Based on the above, Belqis spring can be morphologically and hydro geologically classified as a contact-fault spring. The reservoir rock feeding the spring is the Asmari limestone-karst formation, which occupies part of the outcrop area of the Lar anticline. The height of the spring is 713 meters above sea level. The water flow of the Belqis spring in the water year 2022-2023 fluctuated from about 1.34 cubic meters in February 2022 to.75 cubic meters per second in October 2023. The ratio of its maximum to minimum water flow was calculated to be 1.79 and its average was about 1.04 cubic meters per second. In rainy years, the maximum water flow rate also exceeds 3 cubic meters per second.

The Khemand spring is considered as a representative of the hydrogeological condition of the Sarvak Formation on the southern edge of the Lar anticline. According to the morphological evidence and the drawn structural sections, the Khemand spring is a contact-fault type spring. This spring emerged at a level of 799 meters above sea level in the southeast of the study area, along the transverse fault cutting the Lar anticline. This fault has a northeast-southwest trend. The spring water outlet is discharged from several points in the form of a fracture zone. This spring has little water flow variation, which indicates

the greater role of fractures and matrix in the hydrogeological system of the limestone aquifer that feeds it. The water flow of the Khemand spring in the water year 2022-2023 fluctuates from 0.831 cubic meters per second in February 2022 to 0.265 cubic meters per second in October 2023. The ratio of the maximum water flow to the minimum water flow was calculated to be 1.3 and its average was about 0.46 cubic meters per second. In rainy years, the maximum water flow exceeds 2.5 cubic meters per second.

The catchment area and altitude exit of the springs are given in Table 4. It is evident from Table 4 that catchment area of the Belqis spring is considerably larger with respect to other springs, and this is influencing outflow discharge of the spring. The turbulent and diffuse flow show development of large fissures to conduits and small fractures to fissures in the catchment areas of Belqis, Korsa and Khimand springs respectively. The discharge curves of springs, which are plotted from daily and weekly gauge measurement installed at each spring's location, indicate maximum and minimum discharge of the springs. As shown in Figure 9, the discharge of Belqis and Khimand springs are sustainable throughout the year, while the Korsa spring flows only for few months and dries up after rainfall. The same curves have been used for estimation of dynamic potential of springs and as depicted in Table 4, the Belqis storage potential is appreciable.

Table 4. The physical characteristics of the springs.

Spring	Type	Altitude (m)	Catchment area (km^2)	Discharge (m^3)	Dynamic storage (MCM/Annum)	Quick Flow (%)	Base Flow (%)	Draying Time	α_1	α_2
Belqis	Pseudo-diffuse flow	713	100	0.75–1.34	44	7.3	92.7	271	0.006	0.003
Korsa	Conduit	830	17	0–2.95	7	77.9	22.1	13	0.05	0.01
Khimand	Diffuse-Conduit	799	40	0.26–0.83	16.5	17.8	82.2	82	0.01	0.003

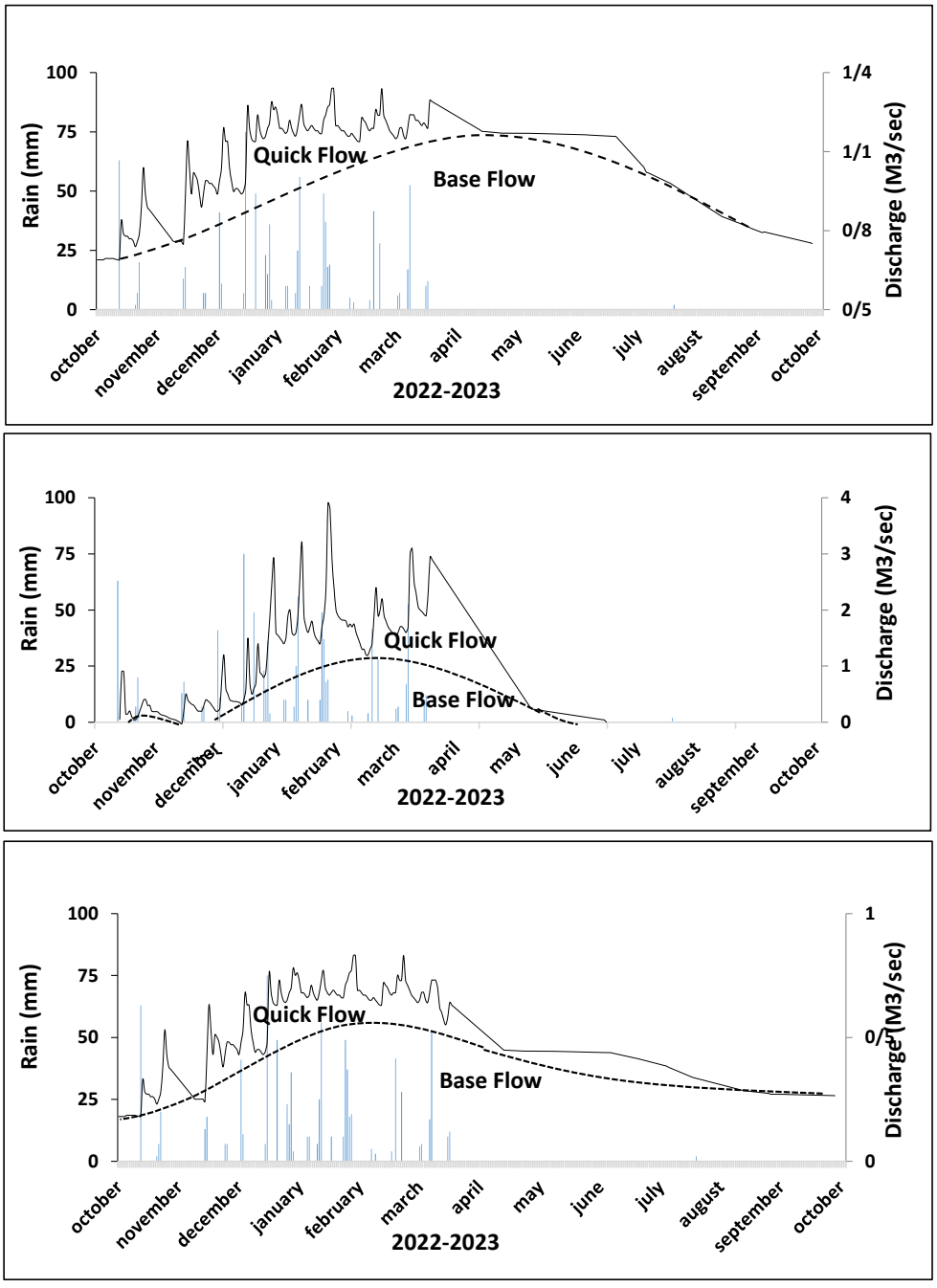

Fig 9. Springs hydrograph a) Belqis b) Korsa c) Khimand.

Conclusion

One of the main factors for karst development in the area is tectonic activity and occurrence of lineaments in various scales. Structural processes are responsible for the three distinct karstic zones development. The hydraulic connection between springs is governed by fault, poljes and ponors. The frequency of longitudinal and lateral fractures trending N45W and N45E respectively in Belqis and

Korsa catchments are significant for aquifers recharge. These fractures are responsible for quick response of aquifers to events. Due to various sources of recharge and the large catchment area, Belqis flows throughout the year while Korsa discharge ends within a short period after rainfall. The fracture development in the Khimand spring tract is less than the springs of Belqis and Korsa and its recharge and discharge are strongly related to open spaces and small fissures. This spring flows throughout the year with minor discharge fluctuation.

In this study, both fuzzy logic-based approach and analytical hierarchy process (AHP) have been used for identifying the areas hierarchy process (AHP) has been used for identifying the areas prone to karstification potentiality in the wider area of Kohgiluyeh and Boyer-Ahmad province. Eight parameters with different weights (lithology, lineament density, elevation, slope, rainfall, temperature, drainage density, and vegetation cover) are used that result into two final maps. The limestones are the geological formations with the highest potentiality for karstification. The very high to high potential zones are characterized by the higher lineament density, higher rainfall, and lithology type such as limestone in most parts of the study area. On the other hand, moderate to poor karstification potential zones are characterized by the lesser lineament density, lower rainfall, lithology type of shale and marl in other parts of the study area. The validity of the illustrated maps is also checked using available data. The validation result shows that the fuzzy logic model has better predication accuracy than the AHP model. Here, the authors conclude that the results of the fuzzy logic model have shown the best prediction accuracy in karstification potentiality mapping in the study area. The maps obtained by these methods can be used by local authorities and water policy makers during periods of drought as a preliminary reference in selecting suitable sites for drilling boreholes. Therefore, the identification of areas, where aquifers are developed can contribute to the rational exploitation, sustainable development of water resources and crisis management in drought conditions. The flexibility of the methods allows the revision of the weights of included parameters, so the methods can be applied in a wider variety of regions.

References

Abbaspour, K. C., Faramarzi, M., Ghasemi, S. S., & Yang, H. (2009). Assessing the impact

of climate change on water resources in Iran. *Water resources research*, *45*(10). https://doi.org/10.1029/2008WR007615

Aghanabati, A. (2004). *Iran's Geology*, Publication of Geology Organization [In Persian]

Alavi, M. (2004). Regional stratigraphy of the Zagros fold-thrust belt of Iran and its proforeland evolution. *American journal of Science*, *304*(1), 1-20.

Antonakos, A. K., Voudouris, K. S., & Lambrakis, N. I. (2014). Site selection for drinking-water pumping boreholes using a fuzzy spatial decision support system in the Korinthia prefecture, SE Greece. *Hydrogeology journal*, *22*(8), 1763-1776. https://doi.org/10.1007/s10040-014-1166-50

Ashjari, J., & Raeisi, E. Z. Z. A. T. (2006). Influences of anticlinal structure on regional flow, Zagros, Iran. *Journal of Cave and Karst studies*, *68*(3), 118-129.

Ayalew, L., & Yamagishi, H. (2005). The application of GIS-based logistic regression for landslide susceptibility mapping in the Kakuda-Yahiko Mountains, Central Japan. *Geomorphology*, *65*(1-2), 15-31. https://doi.org/10.1016/j.geomorph.2004.06.010

Pradhan, B. (2010). Disasters and risk reduction in groundwater: Zagros Mountain, Southwest Iran using geoinformatics techniques. *Disaster Advances*.

Baghvand, A., Nasrabadi, T., Bidhendi, G. N., Vosoogh, A., Karbassi, A., & Mehrdadi, N. (2010). Groundwater quality degradation of an aquifer in Iran central desert. *Desalination*, *260*(1-3), 264-275. https://doi.org/10.1016/j.desal.2010.02.038

Banai-Kashani, R. (1989). A new method for site suitability analysis: The analytic hierarchy process. *Environmental management*, *13*(6), 685-693.

Bastani, M., Kholghi, M., & Rakhshandehroo, G. R. (2010). Modelação inversa de fluxo subterrâneo de densidade variável numa área semi-árida no Irão, usando um algoritmo genético. *Hydrogeology Journal*, *18*, 1191-1203. https://doi.org/10.1007/s10040-010-0599-8

Black, T. J. (1997). Evaporite karst of northern lower Michigan. Carbonates and Evaporites, 12(1), 81-83. https://doi.org/10.1007/BF03175805.

Bonacci, O., Gottstein, S., & Roje-

Bonacci, T. (2009). Negative impacts of grouting on the underground karst environment. *Ecohydrology: Ecosystems, Land and Water Process Interactions, Ecohydrogeomorphology*, *2*(4), 492-502. https://doi.org/10.1002/eco.90.

Bonacci, O., Pipan, T., & Culver, D. C. (2009). A framework for karst ecohydrology. Environmental Geology, 56(5), 891-900. https://doi.org/10.1007/s00254-008-1189-0

Bonacci, O., & Roje-Bonacci, T. (2008). Water losses from the Ričice reservoir built in the Dinaric karst. Engineering Geology, 99(3-4), 121-127. https://doi.org/10.1016/j.enggeo.2007.11.014

Calaforra, J. M., & Pulido-Bosch, A. (2003). Evolution of the gypsum karst of Sorbas (SE Spain). Geomorphology, 50(1-3), 173-180.

Chitsazan, M., Karimi Vardanjani, H., Karimi, H., & Charchi, A. (2015). A comparison between karst development in two main zones of Iran: case study—Keyno anticline (Zagros Range) and Shotori anticline (Central Iran). *Arabian Journal of Geosciences*, *8*(12), 10833-10844. https://doi.org/10.1007/s12517-015-1961-x

Chung, C. J. F., & Fabbri, A. G. (2003). Validation of spatial prediction models for landslide hazard mapping. *Natural hazards*, *30*(3), 451-472. https://doi.org/10.1023/B:NHAZ.0000007172.62651.2b

Cvijić, J. (1898). *Das karstphänomen: Versuch einer morphologischen monographie* (Vol. 2). Hölzel.

De Waele, J., Plan, L., & Audra, P. (2009). Recent developments in surface and subsurface karst geomorphology: An introduction. *Geomorphology*, *106*(1-2), 1-8. https://doi.org/10.1016/j.geomorph.2008.09.023

Döll, P., Lehner, B., & Kaspar, F. (2002, July). Global modeling of groundwater recharge. In *Proceedings of Third International Conference on Water Resources and the Environment Research, Technical University of Dresden, Germany* (Vol. 1, pp. 27-31).

Domakinis, C., Oikonomidis, D., & Astaras, T. (2008). Landslide mapping in the coastal area between the Strymonic Gulf and Kavala (Macedonia, Greece) with the aid of remote sensing and geographical information systems. *International Journal of Remote Sensing*, *29*(23), 6893-6915. https://doi.

org/10.1080/01431160802082130

Entekhabi, D., & Moghaddam, M. (2007). Mapping recharge from space: Roadmap to meeting the grand challenge. *Hydrogeology Journal*, *15*(1), 105-116. https://doi.org/10.1007/s10040-006-0120-6

Echogdali,F.Z.,Boutaleb,S.,Bendarma, A., Saidi, M. E., Aadraoui, M., Abioui, M., ... & Sajinkumar, K. S. (2022). Application of analytical hierarchy process and geophysical method for groundwater potential mapping in the Tata basin, Morocco. *Water*, *14*(15), 2393. https://doi.org/10.3390/w14152393

Field, M. S. (2010). Simulating drainage from a flooded sinkhole. *Acta Carsologica*, *39*(2). https://doi.org/10.3986/ac.v39i2.105

Ford, D. (2007). Jovan Cvijić and the founding of karst geomorphology. *Environmental Geology*, *51*(5), 675-684. https://doi.org/10.1007/s00254-006-0379-x

Ford, D. & Williams, P. (2007). *Karst hydrogeology and Geomorphology*. John Wiley & Sons, New York, Toronto.

Ghayoumian, J., Saravi, M. M., Feiznia, S., Nouri, B., & Malekian, A. (2007). Application of GIS techniques to determine areas most suitable for artificial groundwater recharge in a coastal aquifer in southern Iran. *Journal of Asian Earth Sciences*, *30*(2), 364-374. https://doi.org/10.1016/j.jseaes.2006.11.002

Goldscheider, N., Mádl-Szőnyi, J., Erőss, A., & Schill, E. (2010). Thermal water resources in carbonate rock aquifers. *Hydrogeology Journal*, *18*(6), 1303-1318. https://doi.org/10.1007/s10040-010-0611-3

Groves, C. & Meiman, J. (2005). Weathering, geomorphic work, and karst landscape evolution in the Cave City groundwater basin, Mammoth Cave, Kentucky. *Geomorphology*, *67*, 115–126. https://doi.org/10.1016/j.geomorph.2004.07.008

Haririan, M. (1990). *Iran's Geomorphology*, Publication of Islamic Azad University. [In Persian]

Hosseini, M., Ghafouri, A.M., Amin. M.S.M., Tabatabaei, M.R., Goodarzi, M. & Abde Kolahchi, A. (2012). Effects of land use changes on water balance in Taleghan Catchment, Iran. *Journal of Agric Sci Tech*, *14*, 1159-1172.

Huan, H., Wang, J., & Teng, Y. (2012). Assessment and

validation of groundwater vulnerability to nitrate based on a modified DRASTIC model: a case study in Jilin City of northeast China. *Science of the total environment*, *440*, 14-23. https://doi.org/10.1016/j.scitotenv.2012.08.037

Humphreys, W. F. (2006). Aquifers: the ultimate groundwater-dependent ecosystems. *Australian Journal of Botany*, *54*(2), 115-132. https://doi.org/10.1071/BT04151

Institute of Geological and Mineral Exploration (1967). Geological maps, sheets: Dehdasht, Sisakht and Fahliyan. Scale 1:100.000.

James, G. A., & Wynd, J. G. (1965). Stratigraphic nomenclature of Iranian oil consortium agreement area. *AAPG bulletin*, *49*(12), 2182-2245. https://doi.org/10.1306/A663388A-16C0-11D7-8645000102C1865D

Johnson, S.B. & Stieglitz, R.D. (1990). Karst features of a glaciated dolomite peninsula, Door County, Wisconsin. *Geomorphology*, *4*, 37-54. https://doi.org/10.1016/0169-555X(90)90025-L

Kalantari, N., Ghafari, H. R., Keshavarzi, M. R., & Mallaei, M. R. (2011). Factors impacting on flow pattern in the Shimbar karstic area in the southwest of Iran. In *9 th conference on limestone hydrogeology*.

Karimi, H., Raeisi, E. & Zare, M. (2003). Hydrodynamic Behavior of the Gilan Karst Spring, West of the Zagros, Iran. *Journal of Cave and Karst Science*, *30* (1), 15-22.

Kazakis, N. & Voudouris, K.S. (2015). Groundwater vulnerability and pollution risk assessment of porous aquifers to nitrate: Modifying the DRASTIC method using quantitative parameters. *Journal of Hydrology*, *525*, 13-25. https://doi.org/10.1016/j.jhydrol.2015.03.035

Konkul, J., Rojborwornwittaya, W. & Chotpantarat, S. (2014). Hydrogeologic characteristics and groundwater potentiality mapping using potential surface analysis in the Huay Sai area, Phetchaburi Province, Thailand. *Journal of Geosci*, *18* (1), 89-103. https://doi.org/10.1007/s12303-013-0047-6

Maleki, A., Shoohani, D. & Alaeitaleghani. M. (2009). *Zooning of Karst development in Kermanshah provine*, Modarres seasonal of humanities, 13th course *1*, 272-295 [In Persian]

Magnabosco, R., Galvão, P. &

de Carvalho, M. (2020). An approach to map karst groundwater potentiality in an urban area, Sete Lagoas, Brazil. *Journal of Hydrogeology*, *65*(14), 2482–2498. https://doi.org/10.1080/02626667.2020.1802031

Moghimi, H. (2010). *Karst hydrology*. Publication of Payam-e Noor [In Persian]

Neshat, A., Pradhan, B., Pirasteh, S., & Shafri, H. Z. M. (2014). Estimating groundwater vulnerability to pollution using a modified DRASTIC model in the Kerman agricultural area, Iran. *Environmental earth sciences, 71*(7), 3119-3131. https://doi.org/10.1007/s12665-013-2690-7

Nosrati, K., & Van Den Eeckhaut, M. (2012). Assessment of groundwater quality using multivariate statistical techniques in Hashtgerd Plain, Iran. *Environmental Earth Sciences*, *65*(1), 331-344. https://doi.org/10.1007/s12665-011-1092-y

Pourghasemi, H. R., Pradhan, B., & Gokceoglu, C. (2012). Application of fuzzy logic and analytical hierarchy process (AHP) to landslide susceptibility mapping at Haraz watershed, *Iran. Natural hazards*, *63*(2), 965-996. https://doi.org/10.1007/s11069-012-0217-2

Rahmati, O. (2013). *An investigation of quantitative zonation and groundwater potential (case study: Ghorveh-Dehgolan plain)* (Doctoral dissertation, Tehran University). [In Persian].

Ravbar, N., & Goldscheider, N. (2007). Proposed methodology of vulnerability and contamination risk mapping for the protection of karst aquifers in Slovenia. *Acta carsologica, 36*(3). https://doi.org/10.3986/ac.v36i3.174

Saaty, T. L. (1980). The analytic hierarchy process.

Saaty, T. L. (1977). A scaling method for priorities in hierarchical structures. *Journal of mathematical psychology*, *15*(3), 234-281. https://doi.org/10.1016/0022-2496(77)90033-5

Saaty, T. L. (2001). Models, methods, concepts & applications of the analytic hierarchy process.

Taşci, S., Şenocak, S., Doğru, F., Wang, B., Abdelrahman, K., Fnais, M. S., & El-Raouf, A. A. (2025). Geospatial and multi-criteria analysis for identifying groundwater potential zones in the Oltu basin, Turkey. *Water*, *17*(2), 240. https://doi.

org/10.3390/w17020240

Tweed, S. O., Leblanc, M., Webb, J. A., & Lubczynski, M. W. (2007). Remote sensing and GIS for mapping groundwater recharge and discharge areas in salinity prone catchments, southeastern Australia. *Hydrogeology Journal*, *15*(1), 75-96. https://doi.org/10.1007/s10040-006-0129-x

Vigna, B., Fiorucci, A., Banzato, C., Forti, P., & De Waele, J. (2010). Hypogene gypsum karst and sinkhole formation at Moncalvo (Asti, Italy). *Zeitschrift für Geomorphologie. Supplementband*, *54*(2), 285. http://doi.org/0.1127/0372-8854/2010/0054S2-0015

Yeh, H. F., Cheng, Y. S., Lin, H. I., & Lee, C. H. (2016). Mapping groundwater recharge potential zone using a GIS approach in Hualian River, Taiwan. *Sustainable Environment Research*, *26*(1), 33-43. https://doi.org/10.1016/j.serj.2015.09.005

Zadeh, L. A. (1965). Fuzzy sets. *Information and control*, *8*(3), 338-353. https://doi.org/10.1016/S0019-9958(65)90241-X

Zarghami, M., Abdi, A., Babaeian, I., Hassanzadeh, Y., & Kanani, R. (2011). Impacts of climate change on runoffs in East Azerbaijan, Iran. *Global and Planetary Change*, *78*(3-4), 137-146. https://doi.org/10.1016/j.gloplacha.2011.06.003